

THE INTRACLUSTER PLASMA: A UNIVERSAL PRESSURE PROFILE?

A. LAPI^{1,2}, A. CAVALIERE^{1,3}, R. FUSCO-FEMIANO⁴

¹Dip. Fisica, Univ. ‘Tor Vergata’, Via Ricerca Scientifica 1, 00133 Roma, Italy.

²SISSA, Via Bonomea 265, 34136 Trieste, Italy.

³INAF, Osservatorio Astronomico di Roma, via Frascati 33, 00040 Monteporzio, Italy and

⁴INAF-IASF, Via Fosso del Cavaliere, 00133 Roma, Italy.

Accepted by ApJL

ABSTRACT

The pressure profiles of the Intracluster Plasma in galaxy clusters show a wide variance when observed in X rays at low redshifts $z \lesssim 0.2$. We find the profiles to follow two main patterns, featuring either a steep or a shallow shape throughout both core and outskirts. We trace these shapes back to a physical dichotomy of clusters into two classes, marked by either low entropy (LE) or high entropy (HE) throughout. From X-ray observations and Sunyaev-Zel’dovich stacked data at higher $0.2 \lesssim z \lesssim 0.4$, we elicit evidence of an increasing abundance of HEs relative to LEs. We propose this to constitute a systematic trend toward high z ; specifically, we predict the pressure profiles to converge into a truly universal HE-like template for $z \gtrsim 0.5$. We submit our physical templates and converging trend for further observational tests, in view of the current and upcoming measurements of individual, stacked, and integrated Sunyaev-Zel’dovich signals.

Subject headings: cosmic background radiation — galaxies: clusters: general — X-rays: galaxies: clusters — methods: analytical

1. INTRODUCTION

A keen interest is focusing on the radial pressure profiles $p(r)$ that prevail in the hot intracluster plasma (ICP) filling up the galaxy clusters. Specifically, it is debated the degree of their ‘universality’ among rich clusters, on the following grounds.

On the upside, the profile of the ICP thermal pressure $p \equiv nk_B T/\mu$ (with the mean molecular weight $\mu \approx 0.59$ for cosmic abundances) is expected to score off the components: temperature $T(r)$ and number density $n(r) \equiv \rho(r)/m_p$, on account of its prompt equilibration at sound speed in the absence of forcing stresses. The equilibrium gradient is simply linked by

$$\frac{dp}{dr} = -\frac{GM(<r)}{r^2} \rho \quad (1)$$

to the gravitational force from the dark matter (DM) distribution $M(<r)$ on the ICP mass density ρ .

On the downside, one may worry that the equilibrium pressure profiles might be affected by the *complexities* elicited for redshifts $z \lesssim 0.2$ in the X-ray observations. These probe n from the surface brightness $S_X \propto n^2 T^{1/2}$ emitted by the ICP via thermal bremsstrahlung, while the temperatures $k_B T$ in the keV range are measured from spectroscopy.

In fact, in the cluster cores for $r \lesssim 0.2 R_{500}$ ¹ the radiation observed in X rays is to erode the ICP thermal content on the cooling timescale $t_c \approx 30 (k_B T/\text{keV})^{1/2} (n/10^{-3} \text{ cm}^{-3})^{-1} \text{ Gyr}$ (e.g., White & Rees 1978; Voit & Bryan 2001). The process tends to speed up as n

raises and T lowers, to the effect of steepening the inner pressure gradient after Eq. (1). A catastrophic runaway is conceivably offset by the energy fed back from self-regulated AGN activities (see discussions by Cavaliere et al. 2002; Lapi et al. 2003, 2005; Ciotti & Ostriker 2007; Churazov 2010), or is even forestalled by strong energy injections from deep mergers (see McCarthy et al. 2007; Markevitch & Vikhlinin 2007).

In the cluster outskirts for $r \gtrsim R_{500}$, a pressure jump is forced by shocks driven by the supersonic inflow of cold external gas. Thus the gravitational infall energy is mainly thermalized at the virial boundary (see Lapi et al. 2005, 2010; Voit et al. 2005); meanwhile, part of it drives outer subsonic turbulence contributing to the equilibrium so as to require lower thermal pressures (see Lau et al. 2009; Cavaliere et al. 2011a).

Bypassing such complexities, a ‘universal’ fitting formula for the pressure profiles has been proposed by Nagai et al. (2007) to interpret the outcomes of hydrodynamical simulations of relaxed clusters (see also Battaglia et al. 2011), and applied by Arnaud et al. (2010) to render with empirically adjusted parameters the X-ray data out to R_{500} for $z \lesssim 0.2$. Actually, these analyses led to recognize an average profile along with a considerable *variance*.

On the other hand, the pressure profiles can be *directly* probed with the thermal Sunyaev-Zel’dovich effect (1980; SZ) that occurs as CMB photons are inverse Compton scattered by the hot ICP electrons, and change the radiation temperature $T_{\text{cmb}} \approx 2.73 \text{ K}$ by an amount $\Delta T = g_\nu y T_{\text{cmb}} \sim -0.5 \text{ mK}$. This provides a linear, intrinsically z -independent probe of the thermal electron pressure $p_e = \mu p/\mu_e \approx 0.52 p$ (with the mean molecular weight per electron $\mu_e \approx 1.15$), since its strength is given by the Comptonization parameter $y \equiv (\sigma_T/m_e c^2) \int dl p_e(r) \sim 10^{-4}$ integrated along the l.o.s. The spectral factor g_ν approaches the value -2 at

¹ We adopt the flat cosmology with matter density parameter $\Omega_M = 0.3$, Hubble constant $H_0 = 70 \text{ km s}^{-1} \text{ Mpc}^{-1}$, and mass variance $\sigma_8 = 0.8$ (Komatsu et al. 2011). The virial radius reads $R \approx R_{100} \approx 4 R_{200}/3 \approx 2 R_{500}$ in terms of the radii encircling average overdensities 100, 200 and 500 over the critical density, and takes on values around 2 Mpc for rich clusters.

low frequencies (see Rephaeli 1995); its positive signature for $\nu > 217$ GHz offers a powerful cross-check for the SZ nature of the signals.

The SZ observations now start to probe the radial profiles in nearby individual clusters, and in more distant stacked samples (*SPT* collaboration, Plagge et al. 2010; *WMAP* collaboration, Komatsu et al. 2011; *Planck* collaboration, Aghanim et al. 2011a, 2011b). They are also addressing the cluster contribution to the CMB power spectrum at multipoles $\ell \gtrsim 2000$ (see Lueker et al. 2010; Dunkley et al. 2011; Reichardt et al. 2011). Extensive data at higher resolutions and sensitivities are expected from current and upcoming instrumentation, and eventually from *ALMA* (see Birkinshaw & Lancaster 2007). All such actively pursued observations call for a reliable template to interpret and assess their astrophysical and cosmological import.

Here we take advantage of the effective formalism provided by the Supermodel (SM; Cavaliere et al. 2009, Fusco-Femiano et al. 2009, see <http://people.sissa.it/~lapi/Supermodel/>) to show that the complex ICP thermal states still allow a neat *physical* description of the spherically-averaged pressure profiles. In response to the intriguing challenge posed by Arnaud et al. (2010), we find *two* basic shapes to span the observed variance in the pressure profiles for low $z \lesssim 0.2$, and predict that they are to converge into a closely *universal* one for high $z \gtrsim 0.5$.

2. A PHYSICAL APPROACH TO PRESSURE PROFILES

In singling out the ICP disposition and evolution we base on the updated paradigm for the hierarchical formation of the containing DM halos (e.g., Zhao et al. 2003; Genel et al. 2010; Wang et al. 2011). The paradigm comprises an early collapse punctuated by major mergers, building up the core over a few crossing times; this occurs at redshifts $z_f \approx 1.5 - 0.5$ weakly depending on the mass $M \sim 10^{14} - 10^{15} M_\odot$. Slow, dwindling inflows of external matter follow over several Gyrs, and accrue the outskirts out to the current virial R in closely stationary conditions described by the Jeans equation. In the process, the core scale radius r_{-2} stays put while R expands, and the ‘concentration’ parameter $c \equiv R/r_{-2}$ correspondingly grows.

The ICP forms from intergalactic gas with pressure $\lesssim 10^{-3}$ eV cm $^{-3}$ (see Ryu et al. 2008; Nicastro et al. 2010) that – along with the DM – inflows at supersonic Mach numbers $\mathcal{M} \gtrsim 10$. The gas is shock-heated at about R , and its pressure jumps by factors $4\mathcal{M}^2 \gtrsim 500$ up to the ICP values $p_R \gtrsim 1$ eV cm $^{-3}$. Inward of R , the pressure rises to balance the DM gravitational pull as described by Eq. (1), with the following *universal* features: the rise will be monotonic within a smooth potential well; the gradient will vanish at the center when the gravitational force does, as implied by the Jeans equilibrium and found in simulations and real data (see Lapi & Cavaliere 2009a, 2009b; Navarro et al. 2010; Newman et al. 2011); the rise terminates with a finite central value, proportional to the thermal energy density.

Within such universal constraints, a full description of the pressure profile is keyed to the specific ‘entropy’ (adiabat) run $k(r) \equiv k_B T/n^{2/3}$ embodying the ICP thermal

state. In fact, using $n \propto (p/k)^{3/5}$ Eq. (1) solves to yield

$$p(r) = \left[p_R^{2/5} + \frac{2}{5} \int_r^R dx \frac{m_p G M(< x)}{x^2 k^{3/5}(x)} \right]^{5/2}, \quad (2)$$

in the context of the SM (see Lapi et al. 2005; Cavaliere et al. 2009). For the DM mass distribution $M(< r)$ we use our α -profiles; these solve the Jeans equations under physical boundary conditions, and agree well with N -body simulations (see Lapi & Cavaliere 2009a).

The key role is played by the entropy run $k(r)$ over scales larger than some 10^2 kpc, for which physical insight is provided by the above picture of cluster formation. The latter indicates the basic *shape* (see also Voit 2005)

$$k(r) = k_c + k_R (r/R)^a; \quad (3)$$

this involves the boundary scales R and k_R , and features two *intrinsic* parameters: the central level k_c , and the average outer slope a . These are evaluated as follows.

In the cluster core $r \lesssim 0.2 R_{500}$ a level $k_c \sim 10^2$ keV cm 2 is set by the early collapse; this results from densities $n \sim 10^{-3}$ cm $^{-3}$ compressed by the standard contrast factor 200 over the average background’s, and from temperatures impulsively raised to values $k_B T \sim GM(< r)/10r \sim$ a few keVs. Thereafter, radiative cooling competes with energy injections from AGNs or mergers to the effect of stabilizing or even raising the time-integrated k_c at levels that gather around 10^1 or 10^2 keV cm 2 (see Cavagnolo et al. 2009; Pratt et al. 2010; Hudson et al. 2010). From Eqs. (1) and (2) the central pressure is seen to follow the basic scalings $p_c \propto k_c^{-5/8}$ and $dp^{2/5}/dr \propto k_c^{-3/5}$.

At the other end $r \gtrsim R_{500}$, an entropy ramp rises with slope $a \lesssim 1.1$, originated by the continuously shocked infall and the progressive stratification of the accreted shells during the slow outskirts growth (see Tozzi & Norman 2001; Lapi et al. 2005). The ramp ends up at the boundary R with the value $k_R \gtrsim 10^3$ keV cm 2 set by strong shocks (see Cavaliere et al. 2011b). From Eqs. (1) and (2) the outer pressure profile follows the basic scaling $p(r) \simeq p_R (r/R)^{-5+2a}$, see Cavaliere et al. (2011b). We stress that $p(r)$ will decrease monotonically outwards even when the temperature $T(r) \propto p^{2/5}(r) k^{3/5}(r)$ features a middle peak at $r \approx 0.2 R_{500}$ due to the entropy rising steeply from a low k_c ; the peak is the defining mark of cool-core clusters (see Molendi & Pizzolato 2001; Lecardi et al. 2010).

When the X-ray data on brightness and temperature of clusters at $z \lesssim 0.2$ are analyzed with the SM, a direct *correlation* between k_c and a emerges (see Cavaliere et al. 2011b). This implies that clusters can be parted into two main classes: LE or HE, featuring low or high entropies, respectively, *throughout* cores and outskirts. The LEs (e.g., A2204, A1795) are marked by low central entropies $k_c \sim 10^1$ keV cm 2 along with shallow entropy slopes $a \lesssim 0.7$; the HEs (e.g., A1656, A399) are marked by higher central values $k_c \gtrsim 10^2$ keV cm 2 along with steeper slopes $a \approx 1$.

Then from the above inner and outer scalings $dp^{2/5}/dr \propto k_c^{-3/5}$ and $p \propto r^{-5+2a}$, we find the pressure profiles to *differ* from HEs to LEs, with the former featuring quite *shallower* gradients both in the core and

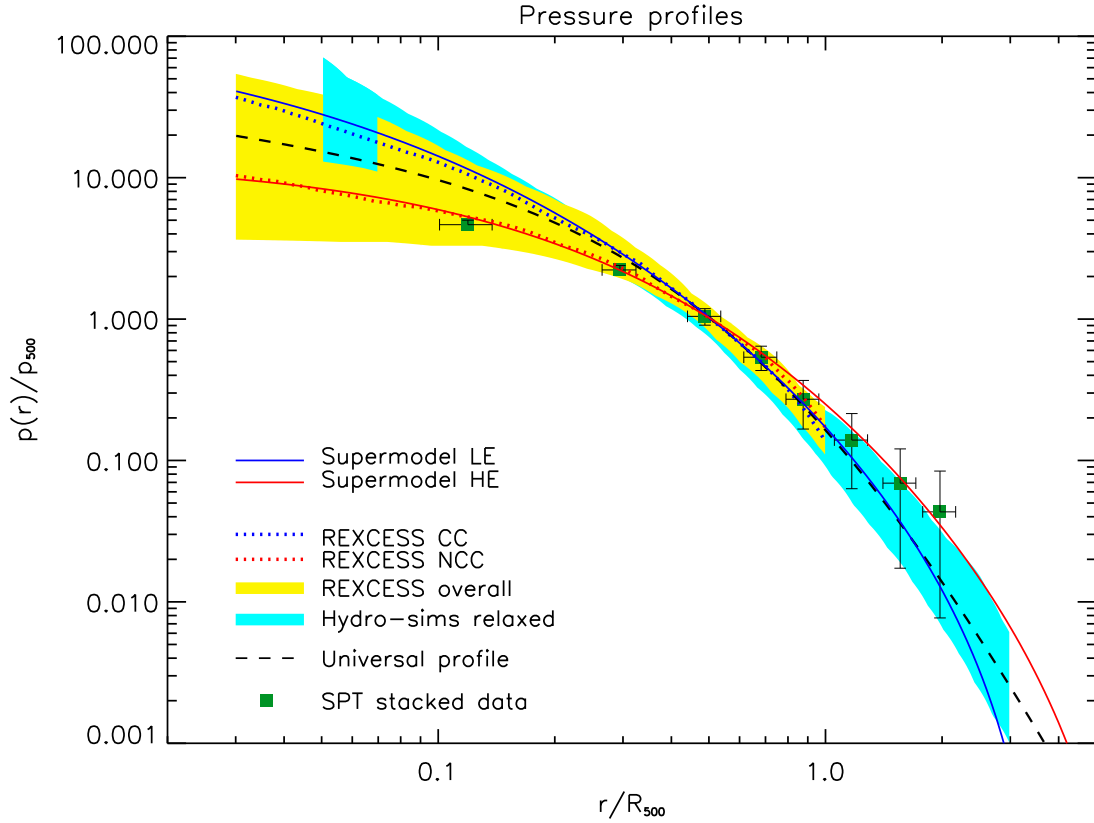


Figure 1. Profiles of ICP pressure normalized to p_{500} , see § 3 for details. The yellow shaded area illustrates the region covered by the low redshift ($z \lesssim 0.2$) clusters of the *REXCESS* X-ray sample; the dotted blue and red lines refer to the average profiles for the subsamples of cool-core and non-cool-core clusters, separately. The cyan shaded area illustrates the coverage by hydrodynamical simulations of relaxed clusters. The dashed line represents the joint fit to the observational and virtual data with the ‘universal’ pressure profile. The green squares represent stacked SZ observations of higher redshift ($0.2 \lesssim z \lesssim 0.4$) clusters with the *SPT*. Our SM templates for HE and LE clusters are illustrated by the red and blue solid lines, respectively.

in the outskirts. Our picture is substantiated by the data presented in Fig. 1.

3. PROBING PRESSURE WITH X RAYS AND SZ EFFECT

In Fig. 1 we compare the pressure profiles computed with our SM to data from X-ray and SZ observations, and from numerical simulations. In the plot, the radial scale is normalized to R_{500} , while the pressure is normalized to the standard value $p_{500} \approx 1.8 h_z^{8/3} (M_{500}/5 \times 10^{14} M_\odot)^{2/3} \text{ eV cm}^{-3}$ in terms of the Hubble parameter $h_z \equiv H(z)/H_0$ (e.g., Ettori et al. 2004; Arnaud et al. 2010).

Our pressure templates provided by Eq. (2) for HE and LE clusters are illustrated by the red and blue solid lines; these are computed from Eqs. (2) and (3) with the parameter values discussed in § 2. Specifically, for typical HEs we adopt $k_c = 100 \text{ keV cm}^2$, $k_R = 3 \times 10^3 \text{ keV cm}^2$ and $a = 1.1$, while for LEs we adopt $k_c = 10 \text{ keV cm}^2$, $k_R = 10^3 \text{ keV cm}^2$, and $a = 0.7$; for both we set $R = 2 \text{ Mpc}$. These values are consistent with the outcomes from detailed SM fits to X-ray observations of nearby clusters carried out by Fusco-Femiano et al. (2009) and Cavaliere et al. (2011b); note, however, that fitting the centrally flat profiles of HEs (e.g., A2256) requires the level k_c to extend out to $r_f \sim 10^2 \text{ kpc}$, bearing the imprint of a recent merger.

The yellow shaded area illustrates the region covered

by the low redshift ($z \lesssim 0.2$) clusters of the *REXCESS* X-ray sample analyzed by Arnaud et al. (2010); the dotted blue and red lines refer to their average profiles for the subsamples of cool-core and non-cool-core clusters, respectively. The cyan shaded area illustrates the region covered by hydrodynamical simulations of relaxed clusters (Borgani et al. 2004; Nagai et al. 2007; Piffaretti & Valdarnini 2008; Battaglia et al. 2011).

The dashed line represents the joint fit by Arnaud et al. (2010) to the observational and virtual data in terms of their ‘universal’ pressure profile. For $r \lesssim R_{500}$ the X-ray data show that such a profile yields only an average but incomplete description. In fact, the partial averages over the cool-core and non-cool-core subsamples deviate upward and downward by a large amount exceeding their internal variance; thus a *bimodal* description constitutes both a closer and a more effective representation. This is just what is provided by the above SM templates for HE or LE clusters, which in the core recover the non-cool-core or cool-core behaviors. Moreover, for $r \gtrsim R_{500}$ where only scarce X-ray data are available, the SM template for LE clusters agrees well with the results of hydro-simulations of relaxed clusters. In the way of a *prediction*, beyond R_{500} we expect for HEs considerably higher pressure profiles relative to LEs, as represented in Fig. 1.

In addition, our picture envisages for decreasing z an

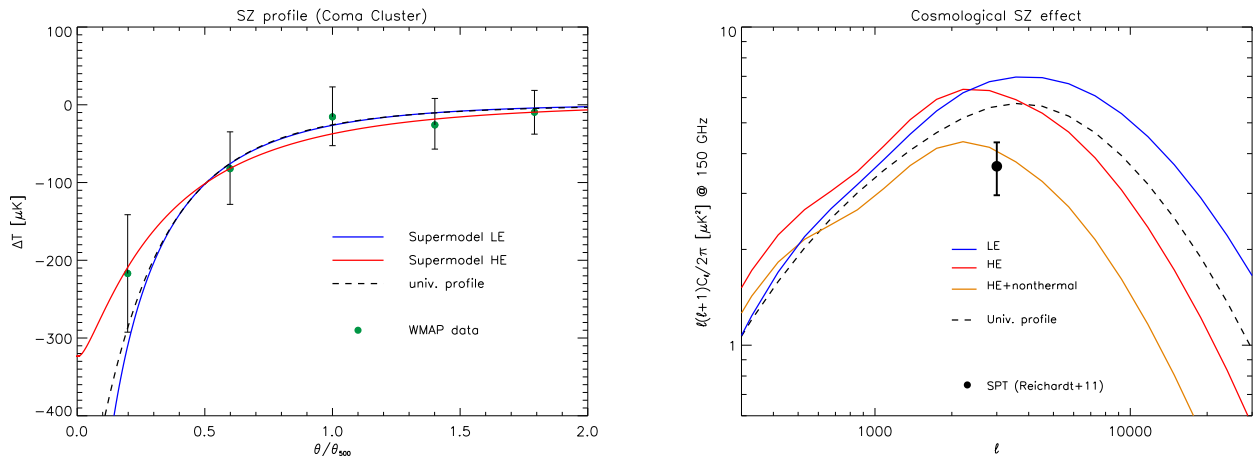


Figure 2. *Left panel:* Profile of the SZ signal from the Coma Cluster, in terms of Rayleigh-Jeans temperature decrement ΔT . The green filled dots illustrate the WMAP data. The black dashed line refers the ‘universal’ pressure profile. The red and blue solid lines illustrate our SM outcomes for HE and LE clusters. *Right panel:* Cosmological thermal SZ effect at 150 GHz. The black dot with error bars illustrates the current constraints set with the SPT. The dashed line refers to the ‘universal’ pressure profile. The outcomes from our SM templates are illustrated by the solid lines: blue for LEs, red for HEs, and orange for HEs with a nonthermal component increasing with z (see § 3).

ICP evolution from HE to LE states. In fact, over lifetimes of several Gyrs elapsed from the formation $z_f \approx 1$ to the observation redshift $z \lesssim 0.2$ the outer slope a will flatten out from values $a \approx 1.1$ towards values $a \lesssim 0.5$, and correspondingly the boundary level k_R decreases; such a trend is enhanced as z approaches 0, when the cosmic timescale lengthens considerably. This is because the entropy production by weakened virial shocks is *reduced* as inflows peter out, especially in the accelerated cosmology (see Lapi et al. 2010). Meanwhile, cooling *erodes* the central entropy k_c over comparable times $t_c \approx 5(k_c/100 \text{ keV cm}^2)^{1.2}$ Gyr after Eq. (2), and undergoes an accelerated drop toward the ‘attractor’ level $k_c \sim 10 \text{ keV cm}^2$ set by competition with AGN feedback.

On the other hand, the evolution of the cluster DM halo is marked by the growth of the ‘concentration’ $c \approx 3.5 h_{z_f}/h_z$ from z_f to z (see Zhao et al. 2003; Prada et al. 2011). Since a and k_c decrease together, we expect them both to *anticorrelate* with c . In fact, such correlations a, k_c vs. c^{-1} have been quantitatively elicited with SM analyses of high-quality X-ray data concerning several clusters at $z \lesssim 0.2$ (see Cavaliere et al. 2011b).

As z increases, our evolutionary trend envisages the HE/LE ratio to grow towards 1; in other words, we expect all pressure profiles to converge toward a truly *universal* template provided by the HE shape. Our picture is supported by comparison of the local data with stacked SZ observations of redshifts $0.2 \lesssim z \lesssim 0.4$ clusters; the pressure profiles from the SPT stacked data (Plagge et al. 2010) are represented in Fig. 1 with the green squares. Although the uncertainties are still considerable in the outskirts, a departure from the ‘universal’ profile stands out, and the trend toward an HE-like template clearly emerges. The same trend is emerging from the analysis of a stacked cluster sample observed with WMAP (Komatsu et al. 2011). A similar trend is suggested by the sample of clusters detected by Planck for redshift $0.3 \lesssim z \lesssim 0.5$, and followed up in X rays with XMM-Newton (Aghanim et al. 2011b). Independent evidence is provided by the dearth of strong cool-cores found in X rays by Santos et al. (2010) at high-redshifts.

The next step to test the evolutionary trend from LEs to HEs will involve observing the SZ profile from individual clusters over an extended range of redshifts. This is still challenging with the present instrumentation even at $z \lesssim 0.2$, but will become feasible out to high $z \gtrsim 0.5$ with new-generation instruments up to ALMA (see <http://www.almaobservatory.org/>). To illustrate the current status, in Fig. 2 we report the recent data on the SZ profile for the Coma Cluster at $z \approx 0.023$ with WMAP (Komatsu et al. 2011). We also report the ‘universal’ pressure profile (black dashed line), and the Supermodel templates for HE and LE clusters (red and blue solid lines). These data allow to recognize the HE nature of the Coma cluster, still more prominent in X rays. On the other hand, the SZ data will become competitive once resolutions better than $1'$ will be attained.

Another testbed for our evolutionary picture will be provided by the power spectrum of the unresolved SZ effect integrated over redshift and over the evolving cluster mass distribution including groups (e.g., Shaw et al. 2010; Efstathiou & Migliaccio 2011). In Fig. 3 we illustrate the outcome from the ‘universal’ profile of Arnaud et al. (2010) and the SM templates for LE and HE clusters, compared with the constraints at $\ell \sim 3000$ set by current observations with the SPT (Reichardt et al. 2011). The latter are converging to indicate that the integrated SZ effect is to be both dominated by HEs at the relevant $z \gtrsim 0.5$, and reduced by the presence of a nonthermal contribution to the inner ICP equilibrium.

We find consistency of our HE template with the data when the standard scaling $p_{500} \propto h_z^{8/3}$ is decreased by a factor $h_z^{-1/2}$; the latter renders how the inner nonthermal component mildly increases with z , as expected for the early HE equilibrium punctuated by major mergers with strong turbulent wakes (see § 2 and Cavaliere et al. 2011a). Additional constraints on the detailed shape of the SZ effect will require high sensitivities at resolutions $\ell \gtrsim 5000$ with good control of the systematics, an effort actively pursued by the SZ community.

4. DISCUSSION AND CONCLUSIONS

As the observational uncertainties in the SZ measurements are shrinking below the theoretical ones, we have aimed at eliciting truly universal features in the pressure profiles of the Intracluster Plasma (ICP). These are described in terms of our Supermodel, are tested at low z against X-ray observations of brightness and temperature, and are proposed for probing at higher z with the linear, z -independent SZ effect.

At low $z \lesssim 0.2$ we identify from X-ray data two main pressure patterns, each featuring related shapes at the center and in the outskirts. These are interpreted in terms of two cluster classes: HEs with high entropy *throughout*, i.e., high central levels k_c along with a steep outer rise with slope a , leading to shallow pressure profiles; conversely for LEs.

For $z \gtrsim 0.2$ we expect the onset of an evolutionary *trend* in cosmic time from HE to LE, comprising fast erosion of central entropy by radiative cooling, along with reduced outer entropy production by decreasing inflows (see Cavaliere et al. 2011b). Accordingly, the ratio HE/LE is to increase toward high z , implying for $z \gtrsim 0.5$ convergence of the pressure profiles toward a truly *universal*, HE-like template.

Few intermediate instances are expected; these may occur when cooling is forestalled by an exceedingly high initial level $k_c > 10^2$ keV cm², while the outer entropy ramp is independently flattening (e.g., in A1689 and A2218

as discussed by Cavaliere et al. 2011b). On the other hand, Eq. (2) implies our radial pressure profiles to be robust against overall asphericity and localized hot/cold imprints from recent mergers, even when the latter cause wiggles in temperature and marked flatness in the central brightness as often found from detailed fits to X-ray data in HEs (e.g., A2256 as discussed by Fusco-Femiano et al. 2009). This strengthens the case for universality of our asymptotic HE-like pressure template.

We have traced evidence for our evolutionary trend developing in the pressure profiles through stacked SZ signals due to $0.2 \lesssim z \lesssim 0.4$ clusters (see Fig. 1). At higher z , further evidence will be difficult to pinpoint from X rays alone, given their bias toward high central brightnesses proper to LEs; rather, it will be provided again by SZ signals from individual or stacked clusters. In parallel, such an evidence will be tested with the integrated contribution from unresolved SZ signals to the CMB anisotropies at multipoles $\ell \gtrsim 5000$ (see Fig. 2). All such observations require high-sensitivity data at resolutions below $1'$, that are pursued with current instrumentation and will eventually culminate with *ALMA*.

Work supported in part by MIUR, ASI and INAF. We thank M. Massardi, M. Migliaccio, and D. Nagai for helpful discussions, and our referee for useful comments. A.L. thanks SISSA for warm hospitality.

REFERENCES

- Aghanim, N., et al. 2011a, *A&A*, 536, 10
 ——— 2011b, *A&A*, 536, 9
 Arnaud, M., et al. 2010, *A&A*, 517, 92
 Battaglia, N., et al. 2011, *ApJ*, submitted [preprint arXiv:1109.3709]
 Birkinshaw, M., & Lancaster, K. 2007, *NewAR*, 51, 346
 Borgani, S., et al. 2004, *MNRAS*, 348, 1078
 Cavagnolo, K., et al. M. 2009, *ApJS*, 182, 12
 Cavaliere, A., Lapi, A., & Fusco-Femiano, R. 2011b, *ApJ*, 742, 19
 ——— 2011a, *A&A*, 525, 110
 ——— 2009, *ApJ*, 698, 580
 Cavaliere, A., Lapi, A., & Menci, N. 2002, *ApJ*, 581, L1
 Churazov, E. 2010, in *Galaxy clusters: Observations, Physics and Cosmology*, see <http://www.mpa-garching.mpg.de/~clust10>
 Ciotti, L., & Ostriker, J. P. 2007, *ApJ*, 665, 1038
 Dunkley, J., et al. 2011, *ApJ*, 739, 52
 Efstathiou, G., & Migliaccio, M. 2011, *MNRAS*, submitted [preprint arXiv:1106.3208]
 Ettori, S., et al. 2004, *A&A*, 417, 13
 Fusco-Femiano, R., et al. 2009, *ApJ*, 705, 1019
 Genel, S., et al. 2010, *ApJ*, 719, 229
 Hudson, D.S., et al. 2010, *A&A*, 513, 37
 Komatsu, E., et al. 2011, *ApJS*, 192, 18
 Lapi, A., Fusco-Femiano, R., & Cavaliere, A. 2010, *A&A*, 516, 34
 Lapi, A., & Cavaliere, A. 2009a, *ApJ*, 692, 174
 ——— 2009b, *ApJ*, 695, L125
 Lapi, A., Cavaliere, A., & Menci, N. 2005, *ApJ*, 619, 60
 Lapi, A., Cavaliere, A., & De Zotti, G. 2003, *ApJ*, 597, L93
 Lau, E.T., et al. 2009, *ApJ*, 705, 1129
 Leccardi, A., Rossetti, M., & Molendi, S. 2010, *A&A*, 510, 82
 Lueker, M., et al. 2010, *ApJ*, 719, 1045
 Markevitch, M., & Vikhlinin, A. 2007, *Phys. Rep.*, 443, 1
 McCarthy, I.G., et al. 2007, *MNRAS*, 376, 497
 Molendi, S., & Pizzolato, F. 2001, *ApJ*, 560, 194
 Nagai, D., Kravtsov, A. V., & Vikhlinin, A. 2007, *ApJ*, 668, 1
 Navarro J.F., et al. 2010, *MNRAS*, 402, 21
 Newman, A.B., et al. 2011, *ApJ*, 728, L39
 Nicastro, F., et al. 2010, *ApJ*, 715, 854
 Piffaretti, R., & Valdarnini, R. 2008, *A&A*, 491, 71
 Plagge, T., et al. 2010, *ApJ*, 716, 1118
 Prada, F., et al. 2011, *MNRAS*, submitted [preprint arXiv:1104.5130]
 Pratt, G.W., et al. 2010, *A&A*, 511, A85
 Rephaeli, Y. 1995, *ARA&A*, 33, 541
 Reichardt, C.L., et al. 2011, *ApJ*, submitted [preprint arXiv:1111.0932]
 Ryu, D., et al. 2008, *Science*, 320, issue 5878, 909
 Santos, J.S., et al. 2010, *A&A* 521, 64
 Shaw, L.D., et al. 2010, *ApJ*, 725, 1452
 Sunyaev, R.A., & Zeldovich, Ya.B. 1980, *ARA&A*, 18, 537
 Tozzi, P., & Norman, C. 2001, *ApJ*, 546, 63
 Voit, G.M. 2005, *Rev. Mod. Phys.*, 77, 207
 Voit, G.M., & Bryan, G.L. 2001, *Nature*, 414, 425
 Wang, J., et al. 2011, *MNRAS*, 413, 1373
 White, S.D.M., & Rees, M.J. 1978, *MNRAS*, 183, 341
 Zhao, D.H., et al. 2003, *MNRAS*, 339, 12